Conversion of Fibrinogen to Fibrin: Mechanism of Exposure of tPA- and Plasminogen-Binding Sites[†]

Sergei Yakovlev,[‡] Eugeny Makogonenko,[‡,§] Natalia Kurochkina,[‡,||] Willem Nieuwenhuizen,[⊥] Kenneth Ingham,[‡] and Leonid Medved*[,‡]

The American Red Cross Holland Laboratory, 15601 Crabbs Branch Way, Rockville, Maryland 20855, and TNO Prevention and Health, Gaubius Laboratory, P.O. Box 2215, 2301 CE Leiden, The Netherlands

Received August 7, 2000; Revised Manuscript Received October 24, 2000

ABSTRACT: Conversion of fibrinogen into fibrin results in the exposure of cryptic interaction sites and modulation of various activities. To elucidate the mechanism of this exposure, we tested the accessibility of the Aα148−160 and γ312−324 fibrin-specific epitopes that are involved in binding of plasminogen and its activator tPA, in several fragments derived from fibrinogen (fragment D and its subfragments) and fibrin (cross-linked D−D fragment and its noncovalent complex with the E_1 fragment, D−D·E_1). Neither D nor D−D bound tPA, plasminogen, or anti-Aα148−160 and anti-γ312−324 monoclonal antibodies, indicating that their fibrin-specific epitopes were inaccessible. The Aα148−160 epitope became exposed only upon proteolytic removal of the β- and γ-modules from D. At the same time, both epitopes were accessible in the D−D·E_1 complex, indicating that the DD·E interaction resulted in their exposure. This exposure was reversible since the dissociation of the D−D·E_1 complex made the sites unavailable, while reconstitution of the complex made them exposed. The results indicate that upon fibrin assembly, driven primarily by the interaction between complementary sites of the D and E regions, the D regions undergo conformational changes that cause the exposure of their plasminogen- and tPA-binding sites. These changes may be involved in the regulation of fibrin assembly and fibrinolysis.

Fibrinogen (340 kDa) is a multifunctional adhesive protein involved in a number of important physiological and pathological processes. Its multifunctional character is connected with its complex multidomain structure. Fibrinogen consists of two identical subunits, each of which is formed by three nonidentical polypeptide chains, Aα, Bβ, and γ (*1*, *2*). Both subunits and the six chains are linked together by disulfide bonds and assemble to form at least 18 distinct domains grouped into four major structural regions, the central E, two identical terminal D, and αC domains (*3*−*5*). The E region is formed by the NH_2-terminal parts of all six chains, while each D region is formed by the remaining COOH-terminal portions of the Bβ- and γ-chains and a portion of the Aα-chain (*1*, *2*). The D and E regions can be separated by various proteases, resulting in the D and E fragments, respectively (*1*, *6*).

Thrombin-mediated conversion of fibrinogen to fibrin results in spontaneous polymerization of the latter and formation of an insoluble clot that prevents the loss of blood upon vascular injury and serves as a provisional matrix in subsequent tissue repair. The major aspects of the fibrin assembly process were established in numerous studies (*1*, *6*, *7* and references therein). The process is triggered by the removal of fibrinopeptides from the E region and the exposure of two pairs of polymerization sites "A" and "B" (knobs) that associate with complementary sites "a" and "b" (holes) in the D regions (*8*). The noncovalent knob-to-hole (A−a) interaction between one E region and two D regions of individual molecules (DD·E interaction) generates two-stranded protofibrils in which individual monomers are half-staggered with their D regions aligned in an end-to-end manner. The protofibrils associate with each other laterally to produce thicker fibrils that branch to form the fibrin clot. The clot is stabilized by factor XIIIa-catalyzed cross-linking between neighboring D regions. After the fibrin clot has carried out its functions, it is dissolved by the fibrinolytic enzyme plasmin, resulting in soluble degradation products that include the cross-linked dimeric D−D fragment and its noncovalent complex with the E_1 fragment (D−D·E_1 complex) (*6*).

Fibrinogen is rather inert in circulation, but upon conversion into fibrin, it interacts with different proteins and cell types and participates in different physiologically important processes, including fibrinolysis, inflammation, angiogenesis, and wound healing. In contrast to fibrinogen, polymeric fibrin interacts with tissue-type plasminogen activator (tPA),[1] fibronectin, and some cell receptors (*9*−*14*). Such reactivity suggests that during the fibrin assembly process fibrin(ogen) undergoes conformational changes, resulting in the exposure of its multiple interaction sites and modulation of various

[†] This work was supported by National Institutes of Health Grants HL-56051 (to L.M.) and HL-21791 (to K.I.).

* To whom correspondence should be addressed: The Holland Laboratory, American Red Cross, 15601 Crabbs Branch Way, Rockville, MD 20855. Phone: (301) 738-0719. Fax: (301) 738-0794. E-mail: medvedl@usa.redcross.org.

[‡] The American Red Cross Holland Laboratory.

[§] Present address: Institute of Biochemistry, National Academy of Sciences of Ukraine, Kiev 01030, Ukraine.

[||] Present address: School of Theoretical Modeling, P.O. Box 15676, Chevy Chase, MD 20815.

[⊥] Gaubius Laboratory.

10.1021/bi001847a CCC: $19.00 © 2000 American Chemical Society
Published on Web 11/23/2000

activities. The exposure of the tPA- and plasminogen-binding sites on fibrin represents a clear example demonstrating the importance of such conformational changes in the regulation of fibrinolysis. Although plasmin exhibits proteolytic activity toward many plasma proteins, its activity in vivo is restricted mainly to places of fibrin deposition, allowing effective dissolution of the latter without proteolytic damage of other proteins. This important natural adaptation occurs through a number of orchestrated interactions between newly exposed binding sites on fibrin and complementary sites on tPA and plasminogen, resulting in activation of the latter by tPA and localization of fibrinolysis. Similarly, the exposure of some cell binding sites upon fibrin assembly may result in cell adhesion, proliferation, and migration on the fibrin surface.

Changes in fibrinogen conformation can be triggered by different events that often lead to the exposure of the same epitopes as those exposed in fibrin. For example, the interaction of platelet receptor GP IIbIIIa with fibrinogen induces on the latter the exposure of specific receptor-induced binding sites, RIBS (*15*, *16*). The appearance of these epitopes as well as some other fibrin-specific ones could be also induced by adsorption of fibrinogen onto a surface (*16*, *17*). Implanted biomaterials adsorb fibrinogen, and this often results in the increased level of interaction with phagocytic cells via the Mac-1 receptor and the development of chronic inflammation near the implant (*18*, *19*). The exposure of RIBS and Mac-1-, tPA-, and plasminogen-binding sites can also occur upon limited proteolysis, chemical cleavage, and partial denaturation (*9*, *10*, *17*, *20*, *21*).

Although the exposure of fibrin-specific epitopes in the above-mentioned events is well documented, the mechanisms of this exposure remain unknown. A comprehensive understanding of how the conformation of the fibrinogen molecule, especially those regions that are involved in fibrin assembly and various interactions, is changed upon polymerization depends on the availability of a high-resolution three-dimensional structure of fibrinogen. The recently established crystal structure of fibrinogen fragment D and its cross-linked counterpart from fibrin, the D−D fragment (*22*), made it possible to address this question. To elucidate the mechanisms of conformational change in the D regions of fibrinogen upon its conversion to fibrin, we studied the exposure of their fibrin-specific plasminogen- and tPA-binding sites in different model systems that mimic fibrinogen and fibrin. The results indicate that this exposure is caused by conformational changes in the D regions triggered by their interaction with the E region. A detailed mechanism of these changes is proposed.

EXPERIMENTAL PROCEDURES

Proteins. Plasminogen-depleted human and bovine fibrinogen, aprotinin, and bovine serum albumin (BSA) were purchased from Calbiochem. Bovine α-thrombin, plasmin, and streptavidin conjugated to alkaline phosphatase were from Sigma. Recombinant single-chain tPA was a Genentech product known under the trade name "Activase". Glu-plasminogen (form II) was prepared from citrated human plasma by affinity chromatography on Lys-Sepharose 4B (*23*) and further purified by size-exclusion chromatography on Superdex 200.

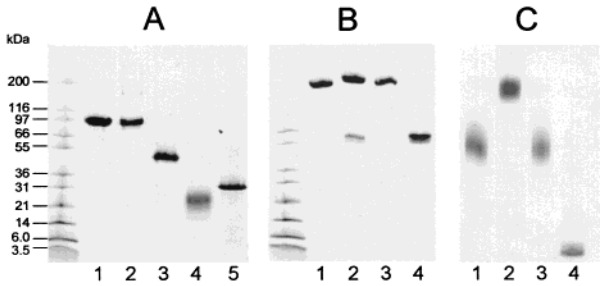

FIGURE 1: Polyacrylamide gel electrophoresis of the fragments used in this study. (A) SDS−PAGE analysis of the D_1, D_H, D_Y, and TSD fragments and the recombinant γ-module (lanes 1−5). Panels B and C represent the PAGE analysis of the D−D fragment isolated from the cross-linked fibrin (lanes 1), the D−D·E_1 complex (lanes 2), and its individual components, D−D (lanes 3) and E_1 (lanes 4), under denaturing [0.55% SDS (B)] and native (C) conditions. The outer lanes in panels A and B contain marker proteins (Mark 12 Unstained Standard, Novex) with the indicated molecular mass.

Fragments. Fibrinogen fragments, human D_1 and bovine D_H, were prepared by procedures described previously (*24*, *25*). The D_H fragment was used as a starting material for preparation of the D_Y and TSD fragments described in refs *25* and *26*. The human fibrinogen γ-module corresponding to γ-chain residues 148−411 was produced in *Escherichia coli* and purified as described previously (*5*). The covalently cross-linked dimeric D fragment (D−D) was prepared from a plasmin digest of factor XIIIa-cross-linked fibrin by the procedure described in ref *27*. All fragments were tested for homogeneity by 8 to 25% SDS−PAGE (Figure 1A,B) and stored frozen at −20 °C. Before each experiment, the D−D, D_1, and D_H fragments were thawed and additionally purified on fibrin−Sepharose as described previously (*28*). Only active fractions that bound to fibrin−Sepharose were used. The noncovalent complex of D−D with the E_1 fragment (D−D·E_1 complex) was obtained as described in ref *27* with some modifications. Namely, after termination of the digestion reaction with aprotinin, plasmin was removed from the digest by affinity chromatography on Lys-Sepharose. The complex was homogeneous as revealed by 12.5% polyacrylamide gel electrophoresis under native conditions (Figure 1C) and size-exclusion chromatography on Superdex 200 (not shown). The NH_2-terminal sequence analysis revealed that it contained mainly the E_1 fragment, and the content of the E_2 fragment never exceeded 20%. Only the freshly prepared complex was used in further experiments.

Dissociation and Reconstitution of the D−D·E_1 Complex. Dissociation of the complex was achieved by the addition of a 10-fold excess of 1 M glycine buffer (pH 3.0), followed by overnight dialysis versus 0.125% acetic acid at 4 °C after which the complex was completely dissociated into individual components as revealed by size-exclusion chromatography on Superdex 200 and polyacrylamide gel electrophoresis under native conditions (not shown). At this stage, a portion of the mixture was applied onto a column with Superdex 200 equilibrated with 20 mM glycine buffer (pH

[1] Abbreviations: tPA, tissue-type plasminogen activator; Pg, plasminogen; BSA, bovine serum albumin; PAGE, polyacrylamide gel electrophoresis; Mab, monoclonal antibody; FITC, fluorescein isothiocyanate; S-2251, H-D-valyl-L-leucyl-L-lysine-*p*-nitroanilide; TBS, 0.02 M Tris buffer (pH 7.4) with 0.15 M NaCl; ϵ-ACA, ϵ-aminocaproic acid; ELISA, enzyme-linked immunosorbent assay; SPR, surface plasmon resonance.

3.5) to separate the D−D and E_1 fragments from each other. The individual fragments were then brought to neutral pH by the addition of a 10-fold excess of 1 M Tris (pH 9.0) and then concentrated with a Centriprep YM-10 filter (Amicon) and dialyzed versus 0.02 M Tris buffer (pH 7.4) with 0.15 M NaCl (TBS). The remaining portion containing the mixture of dissociated D−D and E_1 fragments was brought to neutral pH in the same manner and incubated for 30 min at 37 °C to reconstitute the complex. The formation of the complex was confirmed by the same methods.

Antibodies. Fibrin-specific murine monoclonal antibodies (Mabs) against the Aα148−160 and γ312−324 regions (anti-Aα148−160 Mab and anti-γ312−324 Mab, respectively) were prepared as described previously (*29, 30*). γ-Module-specific sheep polyclonal antibodies against the human fibrinogen γ-module (γ148−411) were kindly provided by Dr. S. Cederholm-Williams (Oxford Bioresearch, Oxford, U.K.). The conjugation of the anti-γ-module antibodies with *N*-hydroxysuccinimide biotin ester (Pierce) was performed by the procedure recommended by the manufacturer.

Preparation of FITC-Labeled Fragments. Fluorescent fragments D_1, D_H, D_Y, and TSD and the γ-module were prepared by labeling with fluorescein isothiocyanate (FITC). The fragments were dialyzed against 0.1 M $NaHCO_3$ (pH 9.5), mixed with a 10-fold molar excess of FITC (Sigma), and incubated for 2 h at 37 °C in the dark. Unreacted dye was removed by chromatography on a Pharmacia NAP-5 Sephadex G-25 prepacked column with subsequent dialysis against 0.1 M HEPES (pH 8.0) containing 1 mM Ca^{2+} and 5 mM octyl glucoside. The degree of labeling was determined spectrophotometrically as described in ref *31* and was found to be 1.7, 1.8, 1.6, 1.3, and 1.5 mol of FITC/mol of D_1, D_H, D_Y, TSD, and the γ-module, respectively.

Chromogenic Substrate Assay. The stimulating effect of fibrin(ogen) fragments on the tPA-catalyzed conversion of plasminogen into plasmin was evaluated by determination of the amidolytic activity of the newly formed plasmin with chromogenic substrate S-2251 (H-D-valyl-L-leucyl-L-lysine-*p*-nitroanilide) (Chromogenix) as described in ref *32*. The assay system contained 0.2 μM Glu-plasminogen, 0.14 nM tPA, 0.3 mM S-2251, and 1 μM fibrin(ogen) fragments in TBS containing 0.05% Tween 80. The assay was performed in the wells of a microtiter plate at 37 °C. The amidolytic activity was determined by measuring the absorbance at 405 nm using a TERMOmax 96-well plate reader (Molecular Devices).

Solid-Phase Binding Assay. Solid-phase binding was performed in a sandwich-type enzyme-linked immunosorbent assay (ELISA). Wells of high-binding microplates (Fisher) were coated overnight at 4 °C with 100 μL of 5 μg/mL anti-Aα148−160 Mab, anti-γ312−324 Mab, or tPA per well in 0.1 M Na_2CO_3 (pH 9.5) (coating buffer). The wells were then blocked with 1% BSA in TBS for 2 h at room temperature. Following washing with TBS containing 0.05% Tween 20 (TBS-T), the indicated concentrations of fibrin(ogen) fragments in TBS-T containing 1 mM Ca^{2+} were added to the wells and also to control wells coated with just BSA and incubated overnight at 4 °C. The binding of these fragments was assessed by the reaction with the biotinylated anti-γ148−411 polyclonal antibodies and streptavidin conjugated to alkaline phosphatase. The alkaline phosphatase substrate, *p*-nitrophenyl phosphate (Sigma) at 1 mg/mL, was added to the wells, and the amount of bound ligand was measured after 20 min spectrophotometrically at 405 nm. Data were fitted by nonlinear regression analysis using eq 1

$$B = B_{max}/(1 + K_d/[L]) \quad (1)$$

where B represents the amount of ligand bound, B_{max} is the concentration of ligand bound at saturation (or the signal proportional to it), [L] is a molar concentration of free ligand, assumed here to be equal to total, and K_d is the dissociation constant.

Biosensor Assay. The interaction of the fibrin(ogen) fragments with tPA, plasminogen, and fibrin-specific monoclonal antibodies, anti-γ312−324 Mab and anti-Aα148−160 Mab, was studied by surface plasmon resonance (SPR) using the IAsys biosensor (Fisons, Cambridge, U.K.) which assesses the association and dissociation of proteins in real time (*33*). The Mabs, tPA, and plasminogen were covalently coupled to the activated carboxymethyl dextran-coated biosensor chip at a coupling density of 9−12 ng/mm^2 by the procedure recommended by the manufacturer. Binding experiments were performed at 25 °C in 50 mM Tris buffer (pH 7.4) containing 1 mM Ca^{2+}, 1% BSA, and 0.05% Tween 20 (binding buffer). The association between the immobilized proteins and the added fibrin(ogen) fragments was monitored as the change in the SPR response. To regenerate the chip, complete dissociation of the complex was achieved by adding 10 mM HCl for 2 min following re-equilibration with binding buffer. The traces of the association process were recorded and analyzed using the FASTfit kinetics analysis software supplied with the instrument as previously described in detail (*34*, *35*). Briefly, the association curves at each concentration of ligand were fitted to the pseudo-first-order equation to derive the observed rate constant (termed the on-rate constant, k_{on}, in FASTfit). Then the concentration dependence of k_{on} was fitted using linear regression to find the association rate constant (k_{ass}) from the slope and dissociation rate constant (k_{diss}) from the intercept. The dissociation equilibrium constant (K_d) was calculated as k_{diss}/k_{ass}. The values were examined for self-consistency of the data as described in ref *36*.

Fluorescence-Detected Binding Measurements. The association of the FITC-labeled fibrinogen fragments with tPA in solution was studied by monitoring the change in fluorescence anisotropy. The anisotropy measurements were performed with an SLM-8000C spectrofluorometer. A concentrated solution of tPA was automatically added with a motor-driven syringe to a stirred cuvette containing the FITC-labeled D species at 0.1 μM while monitoring the anisotropy at 524 nm with excitation at 493 nm. The resulting concentration-dependent increase in anisotropy (A) was fitted to eq 2

$$\Delta A = \Delta A_{max}[L]/(K_d + [L]) \quad (2)$$

where K_d is the dissociation constant and [L] is the concentration of the free ligand. ΔA_{max} was treated as a fitting parameter because the amount of tPA added was not enough to achieve saturation. Since the concentration of labeled proteins was small compared to the K_d, the concentration of free protein was assumed to be equal to the total concentration.

Fluorescence-Detected Unfolding Study. Fluorescence measurements of thermal unfolding were performed by monitoring the ratio of the fluorescence intensity at 370 nm to that at 330 nm with excitation at 280 nm in an SLM 8000-C fluorometer. The temperature was controlled with a circulating water bath programmed to increase the temperature at a rate of ~1 °C/min. The concentration of fibrinogen, fibrin, and fibrin-derived fragments was ~0.04 mg/mL. Fibrin was prepared in the fluorescence cell by mixing 0.04 mg/mL human fibrinogen with 0.01 NIH unit/mL of thrombin followed by incubation at 37 °C for 30 min to form a gel, cooling to 4 °C, and heating to obtain a melting curve.

Protein Structure Analysis. The solvent accessible surface areas of the fibrin-specific epitopes in the fragments D, D−D, and D−D with two different bound ligands were calculated using atomic coordinates that are available from the Brookhaven Protein Database under access codes 1FZA, 1FZB, and 1FZC, respectively (*22*, *37*). All algorithms for protein structure analysis, including determination of the solvent accessible surface area and interatomic contacts, and computer graphics were used from the commercially available MOLE program (Applied Thermodynamics, Hunt Valley, MD).

RESULTS

The Aα148−160 and γ312−324 sequences of the human fibrinogen D region are involved in the binding of tPA and plasminogen and in the stimulation of the tPA-catalyzed activation of the latter (*10*). It was shown that the CNBr fragment FCB-5, which comprises γ312−324, interacts exclusively with tPA in a Lys-independent manner (*38*, *39*), while fragments containing Aα148−160 bind both tPA and plasminogen in a Lys-dependent manner (*40*−*42*). On the basis of these observations and the results of activation studies, it was suggested that in fibrin plasminogen may interact with the Aα-chain site, and tPA with the γ-chain site (*10*, *38*). Here we will refer to Aα148−160 and γ312−324 as plasminogen/tPA (Pg/tPA)- and tPA-binding sites, respectively, or fibrin-specific epitopes since they both are hidden in fibrinogen and become exposed in fibrin as revealed by experiments with monoclonal antibodies against these sequences (*29*, *30*). These epitopes may serve as markers for monitoring the conformational changes that accompany the conversion of fibrinogen to fibrin. To clarify the mechanism of their exposure, we analyzed their accessibility in the fibrinogen-derived D fragment and in the fibrin-derived cross-linked dimeric D−D fragment that were thought to retain the conformation of the corresponding regions in fibrinogen and fibrin, respectively.

Evaluation of the Accessibility of the Aα148−160 Fibrin-Specific Epitope in the D Fragment. The crystal structure of the human fibrinogen D fragment (*22*) revealed that the Aα148−160 epitope is in a helical conformation and represents a part of a triple-helical coiled coil domain (Figure 2A,B). As reported previously (*22*), the Aα148−160 helix is closed off on one side by the β-module, on two others by the β- and γ-helices of the coiled coil, and on its frontside by the fourth helix formed by the 166−195 region of the Aα-chain. It was suggested that upon conversion of fibrinogen to fibrin the fourth helix should be pulled away from the coiled coil to expose the masked residues (*22*). However, one cannot exclude the possibility that the β-module should also be moved away to open up access to Aα148−160 and particularly to residues Val152 and Lys157 which are thought to be important for stimulatory activity (*43*−*46*). To test this possibility, we evaluated the effect of the removal of these structural elements on the accessibility of the Aα148−160 epitope in the D fragment.

Calculation of the solvent accessible surface area of the Aα148−160 region in the D fragment revealed that most of its residues are almost totally buried, having accessible only 0−6% of their surface; only Arg149 has 16% of its surface exposed (Table 1). The removal of the fourth helix (Aα166−195) increases the accessible surface area of 5 of 13 residues; Lys157 remains inaccessible, while the accessibility of Val152 is changed only moderately (from 3 to 9%). In contrast, removal of only the β-module results in a substantial increase in the accessible surface of at least eight residues, including Lys157 (from 0 to 22%) and Val152 (from 3 to 32%) (Table 1). Removal of both regions results in the exposure of three more residues, Glu151, Asp155, and Ile158. Visual examination of the D fragment revealed multiple contacts between side chain residues of the Aα148−160 region and the β-module (Figure 2A). Calculation of the distances between some neighboring residues revealed that Lys157 of the Aα148−160 region is in direct contact with Asp398, Arg415, and Lys428 of the β-module (Figure 2B). Obviously, these multiple contacts provide the interaction between the β-module and the coiled coil domain. The above data suggest that the β-module may play a major role in covering the Aα148−160 epitope in fibrinogen and that the interaction between the coiled coil domain and the β-module must be disrupted and that the latter must be moved away to expose this epitope.

Modulation of the Exposure of the Aα148−160 Epitope by Limited Proteolysis. To test the suggestions presented above, we studied the effect of removing the individual modules from the bovine fibrinogen D_H fragment on the accessibility of its Aα148−160 epitope using tPA, plasminogen, and a specific anti-Aα148−160 monoclonal antibody (Mab) as molecular probes. This fragment is highly homologous to its human analogue, the D_1 fragment (the sequence in the Aα148−160 region is identical), and has a similar fold (*47*). The advantage of using the bovine fragment is that the time course of its proteolysis was well-studied (*26*) and the resulting discrete fragments, D_Y and TSD, were well-characterized (*25*), while analogous fragments from human fibrinogen have not been described. The D_Y fragment occurs upon removal of the γ-module from D_H. Further removal of the β-module results in the TSD fragment that contains only the coiled coil domain, including Aα148−160, and binds plasminogen (*42*) and presumably tPA.

All fragments were labeled with FITC and then titrated with tPA while the fluorescence anisotropy was monitored. No convincing change in anisotropy was detected when the FITC-labeled D_H fragment was titrated with tPA (Figure 3), indicating no interaction and suggesting that in D_H both the Aα148−160 and γ312−324 regions are hidden as in fibrinogen. Similar results were obtained with the human fibrinogen D_1 fragment. At the same time, the anisotropy was changed upon titration with tPA of the FITC-labeled TSD, indicating formation of a complex between them. The changes were reproducible and provided a reliable determi-

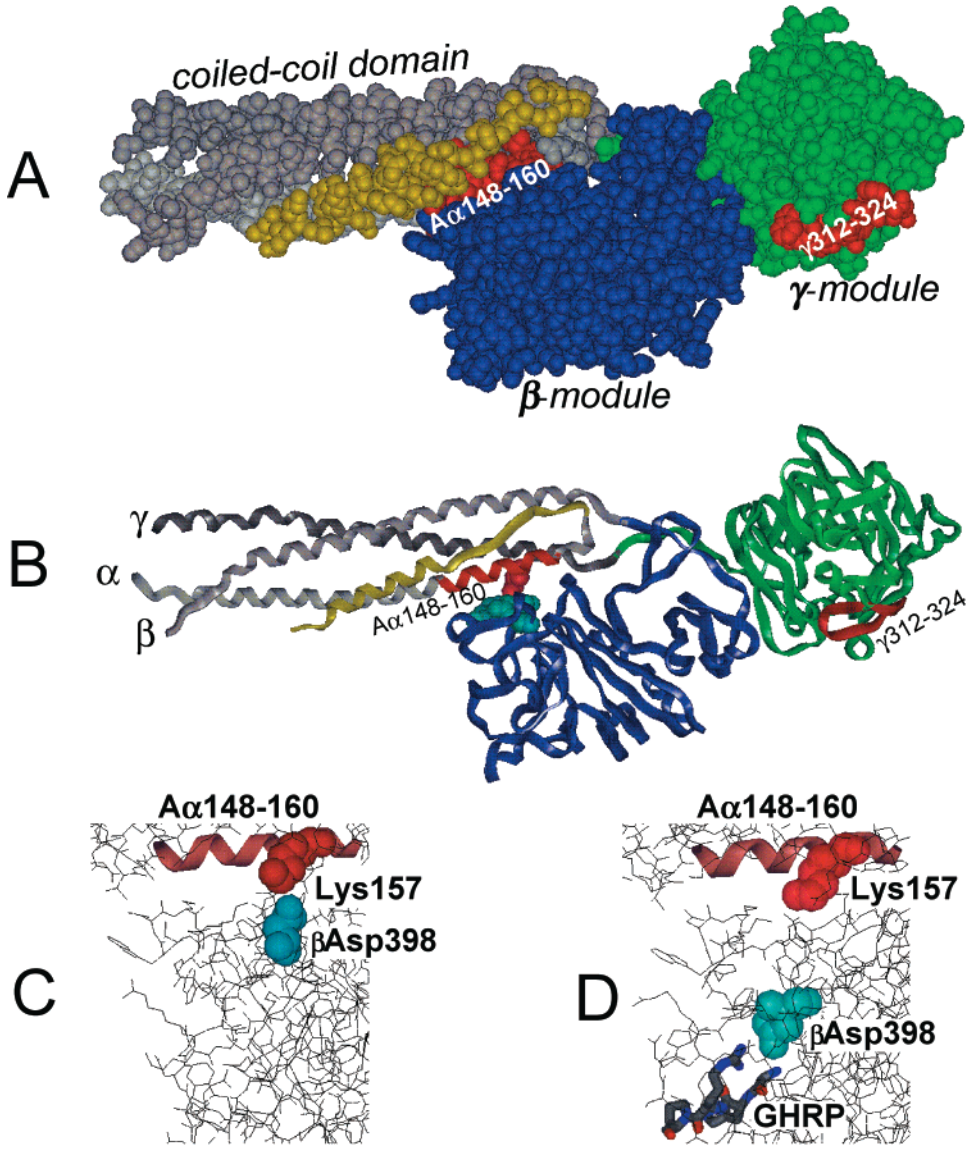

FIGURE 2: Spatial positioning of the fibrin-specific epitopes, Aα148−160 and γ312−324, in the three-dimensional structure of the human fibrinogen D fragment. Panels A and B represent the space-filling model and ribbon diagram of the D fragment based upon its crystal structure, respectively (*22*). The D fragment corresponds to the D region of fibrinogen and includes part of the coiled coil structure formed by all three chains and two homologous modules (β and γ) formed by the COOH-terminal portions of the β- and γ-chains, respectively. The coiled coil domain is in gray; the forth α-helix of the Aα-chain (Aα166−195) is in yellow, and the β- and γ-modules are in blue and green, respectively. The Aα148−160 and γ312−324 regions are in red. Panel B also shows the side chain contacts between Lys157 of the Aα-chain (red balls) and Asp398, Arg415, and Lys428 of the β-module (cyan balls) (see the text). Panel C represents an enlarged view of the contacts between AαLys157 and Bβ Asp398, while panel D shows the positions of these residues in the D−D fragment loaded with the GHRP peptide as reported by Everse et al. (*37*).

nation of K_d (1.2 μM) (Table 2). The complex formation was mediated most probably by the Aα148−160 region, the only one preserved in TSD. The fact that the complex was dissociated when further titrated with ε-aminocaproic acid, ε-ACA, (not shown) is in agreement with the previous report that this site is Lys-dependent (*41*). We performed a similar binding study of tPA with the FITC-labeled D_Y fragment that contains the TSD domain and the β-module but is devoid of the γ-module. The fragment bound tPA in a saturable manner with a K_d of 0.9 μM, similar to that of TSD (Figure 3 and Table 2). Such similarity in K_ds for TSD and D_Y suggests that the binding sites in both fragments are essentially the same.

Binding studies performed by the surface plasmon resonance (SPR) method gave similar results. When tPA was immobilized on a sensor chip, it bound both TSD and D_Y in a dose-dependent manner while no binding was observed with D_H or D_1 (Figure 4A). The binding was blocked by 100 mM ε-ACA. The calculated K_ds for TSD and D_Y were found to be 0.9 and 0.6 μM, respectively, similar to those values obtained in fluorescence experiments (Table 2). When plasminogen was immobilized on a sensor chip, it also bound both TSD and D_Y in a dose-dependent manner while no binding was observed with D_H and D_1 or with TSD and D_Y in the presence of ε-ACA (Figure 4B). The calculated K_d was 1.2 μM for TSD and 1.0 μM for D_Y (Table 2), close to that determined for the TSD fragment earlier by affinity chromatography (*42*). It was also similar to that determined here for tPA. Since in plasma the concentration of plasminogen is more than 4 orders of magnitude higher than that of tPA, this fact reinforces the earlier suggestion (*10*, *38*) that in fibrin, the Aα148−160 region should serve primarily

Table 1: Solvent Accessible Surface Area (%) of the Aα148−160 and γ312−324 Fibrin-Specific Epitopes in the Human Fibrinogen D_1 Fragment and the D−D Dimer

	Aα148−160												
	Lys148	Arg149	Leu150	Glu151	Val152	Asp153	Ile154	Asp155	Ile156	Lys157	Ile158	Arg159	Ser160
D_1	2	16	0	3	3	0	0	1	3	0	0	6	0
D_1 without Aα166−195	48	16	0	30	9	0	2	34	3	0	23	13	0
D_1 without the β-module	20	64	0	3	32	23	0	5	48	22	4	40	43
D_1 without the β-module and Aα166−195	76	64	0	30	43	23	2	40	48	22	23	46	43
D−D with GPRP and GHRP	4	17	1	9	7	1	0	5	4	6	0	14	3
	γ312−324												
	Phe312	Ser313	Thr314	Trp315	Asp316	Asn317	Asp318	Asn319	Asp320	Lys321	Phe322	Glu323	Gly324
D_1	0	0	0	48	37	18	23	18	8	71	29	85	32
D−D with GPRP and GHRP	0	0	0	42	41	17	33	12	8	46	12	78	29

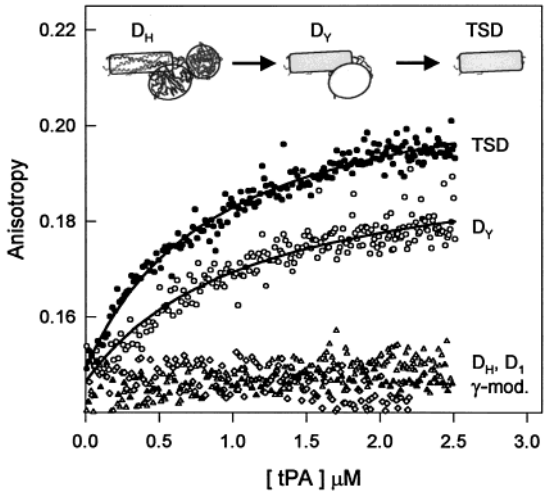

FIGURE 3: Titration of FITC-labeled fragments of fibrinogen with tPA. The FITC-labeled D_1 (▲), D_H (△), D_Y (○), and TSD fragments (●) and the γ-module (◇) at a concentration of 0.1 μM were titrated with tPA in 0.1 M HEPES (pH 8.0) containing 1 mM Ca^{2+} and 5 mM octyl glucoside at 25 °C while monitoring the anisotropy at 524 nm. Curves represent a best fit to eq 2 which yielded the K_d values presented in the text and Table 2. A diagram that defines the fragments used in these experiments is presented at the top.

Table 2: Dissociation Constants[a] for the Interaction of tPA and Plasminogen with Various Fibrin(ogen) Fragments

protein	TSD	D_Y	D_H	D−D·E_1
tPA	1.2 ± 0.3[b]	0.9 ± 0.4[b]	NB[b]	−
	0.9 ± 0.4	0.6 ± 0.2	NB	0.6 ± 0.1
plasminogen	1.2 ± 0.5	1.0 ± 0.1	NB	−

[a] All dissociation constants are in units of micromolar. Values are means ± the standard deviation of three experiments. [b] Obtained by fluorescence anisotropy in fluid phase; remaining values obtained by surface plasmon resonance. NB, no binding detected.

as a plasminogen-binding site. In other SPR experiments when the anti-Aα148−160 Mab was immobilized on a sensor chip, it bound the D_Y and TSD fragments while the level of binding of the D_H fragment was very low (Figure 5). Thus, all the results presented above clearly demonstrate that the Aα148−160 epitope is exposed in both TSD and D_Y fragments. They also indicate that removal of the γ-module from the D_H fragment seems to be sufficient for the exposure of its Aα148−160 epitope, suggesting that the

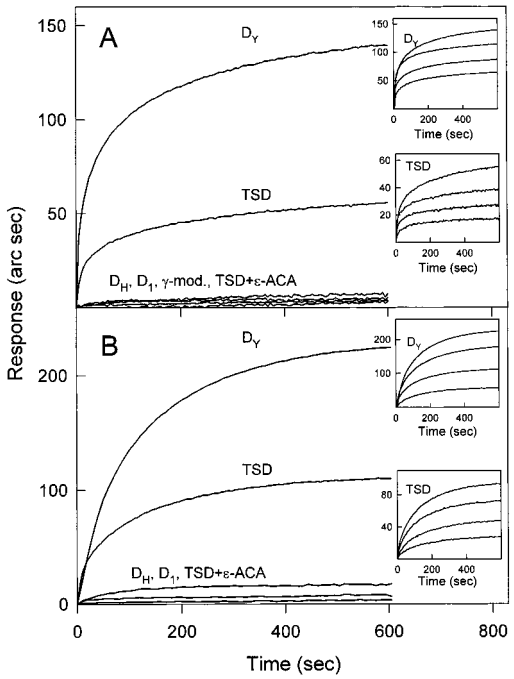

FIGURE 4: Analysis of binding of various fibrinogen fragments to immobilized tPA (A) and plasminogen (B) by surface plasmon resonance. The D_1, D_H, D_Y, and TSD fragments and the γ-module at 2 μM were added to the immobilized tPA (A) or plasminogen (B), and their association was monitored in real time while registering the resonance signal (response). Here and in other figures, a signal of 200 s of arc corresponds to ∼1 ng of protein bound/mm^2 of the sensor chip surface. The binding of D_Y and TSD fragments was dose-dependent as demonstrated in the insets. The concentrations were 0.5, 1.0, 1.5, and 2.0 μM for TSD and 0.25, 1.0, 1.5, and 2.0 μM for D_Y. The K_d values were determined from the association data as described in Experimental Procedures and are presented in the text and Table 2. The curves for the D_H and D_1 fragments, the γ-module, and the TSD fragment in 100 mM ε-ACA presented in both panels essentially coincide.

interaction between the β-module and the coiled coil domain may depend on the status of the γ-module.

The results of the binding studies were well-correlated with the stimulating properties of these fragments in a plasminogen activation assay. When the activation of plasminogen by tPA was monitored by the cleavage of the chromogenic substrate S-2251 with newly formed plasmin, the reaction was much more efficient in the presence of those fragments

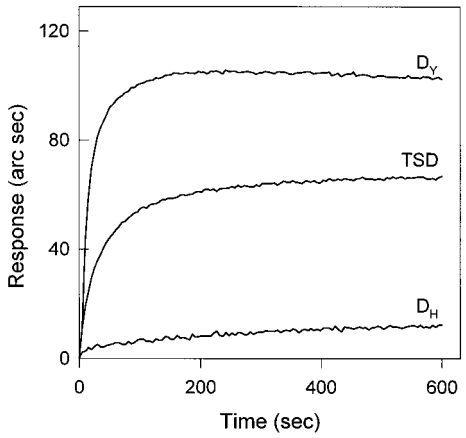

FIGURE 5: Analysis of binding of various fibrinogen fragments to the immobilized anti-Aα148−160 Mab by surface plasmon resonance. The D_H, D_Y, and TSD fragments at 2 μM were added to the immobilized Mab, and their association was monitored in real time while registering the resonance signal (response).

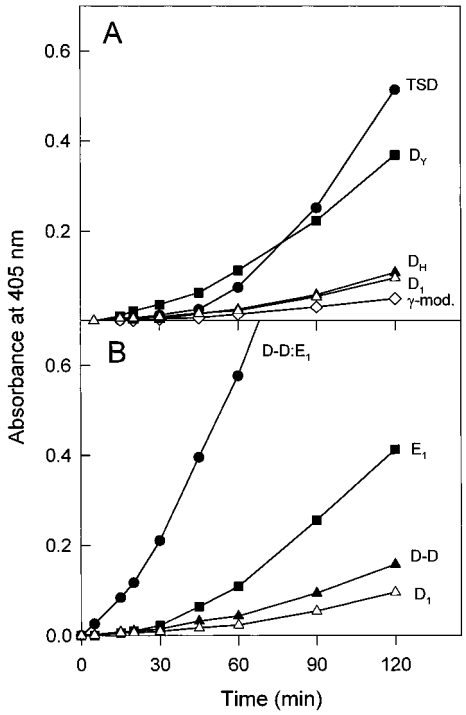

FIGURE 6: Stimulating effect of various fibrin(ogen)-derived fragments on activation of plasminogen by tPA. (A) Stimulating effect of D_1 (△), D_H (▲), D_Y (■), and TSD fragments (●) and the γ-module (◇), each at 1 μM. (B) Stimulating effect of the fibrin-derived D−D (▲) and E_1 (■) fragments and the D−D·E_1 complex (●). The curve for D_1 in panel B is presented for comparison and is essentially the same as the corresponding curve in panel A. The stimulating effect was measured by hydrolysis of the chromogenic substrate S-2251 as described in Experimental Procedures.

that bound tPA in the fluorescence and SPR experiments. The TSD and D_Y fragments stimulated effectively the activation of plasminogen, while the stimulatory effect of the D_H and D_1 fragments was much smaller (Figure 6A). These results together with the binding experiments indicate that the appearance of the stimulating effect in the D_Y and TSD fragments is connected with the exposure of their Aα148−160 epitope.

Evaluation of the Accessibility of the γ312−324 Fibrin-Specific Epitope in the D Fragment. The other fibrin-specific epitope, γ312−324, seems to be more exposed than the Aα148−160 epitope (Figure 2A). In fact, the calculation of its solvent accessible surface area revealed that only three residues (Phe312, Ser313, and Thr314) are totally buried; the rest are pretty much exposed with the highest level of exposure (85%) for Glu323 (Table 1). Such a high degree of exposure suggests that this region should be accessible to tPA and to the specific Mab. However, neither D_H nor D_1 bound tPA in fluorescence or SPR experiments (Figures 3 and 4A). Moreover, the isolated recombinant γ-module (*5*) whose fold is similar to that of the γ-module in the D fragment (*22*, *48*) also failed to bind (Figures 3 and 4A). This suggests that conversion of fibrinogen to fibrin induces conformational changes in the γ-module that either expose the buried residues or alter the disposition of those already exposed to adopt an active tPA-binding conformation.

Modulation of the Exposure of Fibrin-Specific Epitopes by the D−D·E Interaction. Since the D−D fragment derives from polymeric fibrin, one might expect it to preserve the conformation of the D regions of fibrin so that its tPA- and plasminogen-binding sites are exposed. In agreement, it was reported that the D−D fragment retained stimulating capacity and tPA-binding function (*49*, *50*). However, it was also reported that the D−D fragment does not bind tPA− and plasminogen−Sepharose and does not stimulate activation of plasminogen by tPA (*51*, *52*). In our experiments, the D−D fragment exhibited a weak stimulating effect,[2] about double that of D_1 (Figure 6B), consistent with the presence of two D regions in the D−D fragment. At the same time, the noncovalent D−D·E_1 complex, prepared also from cross-linked fibrin, had much higher stimulating activity than the D−D fragment (Figure 6B). Since in the D−D·E_1 complex the D−D fragment interacts with the E_1 fragment via complementary polymerization sites a and A (*6*), this result may suggest that this interaction induces the exposure of the tPA- and plasminogen-binding sites in the D regions. Alternatively, this increased stimulatory effect may be due to the presence of the E_1 fragment in the complex since this fragment itself exhibited a relatively high stimulatory effect (Figure 6B). The first alternative would agree with the recent suggestion that the DD·E interaction is necessary for exposure of fibrin-specific epitopes (*54*), while the second one would support the mechanism suggested by Weitz et al. (*51*), who attributed the stimulating effect of the D−D·E_1 complex to the presence of E_1. To discriminate between these alternatives, we examined the binding of tPA and Mabs specific for the γ312−324 and Aα148−160 epitopes.

We first tested binding of the isolated D−D and E_1 fragments and their D−D·E_1 complex to immobilized tPA by SPR. Negligible binding was observed with the isolated D−D and E_1 fragments, while the D−D·E_1 complex bound to tPA, suggesting that its tPA-binding sites are exposed (Figure 7A). The level of binding was dose-dependent (not

[2] This effect varied for different preparations. At the same time, when the preparations were additionally purified on fibrin−Sepharose and immediately used for study, the effect was reduced and no variability was observed, suggesting the presence in the starting material of the D−D fragment with altered conformation that did not bind to fibrin−Sepharose and could be responsible for the increased stimulating effect. It should be mentioned in this respect that freeze-drying or the presence of EDTA increases the stimulatory effect of fibrinogen (*53*). Thus, proper handling of the D−D fragment upon preparation seems to be important for obtaining reproducible results.

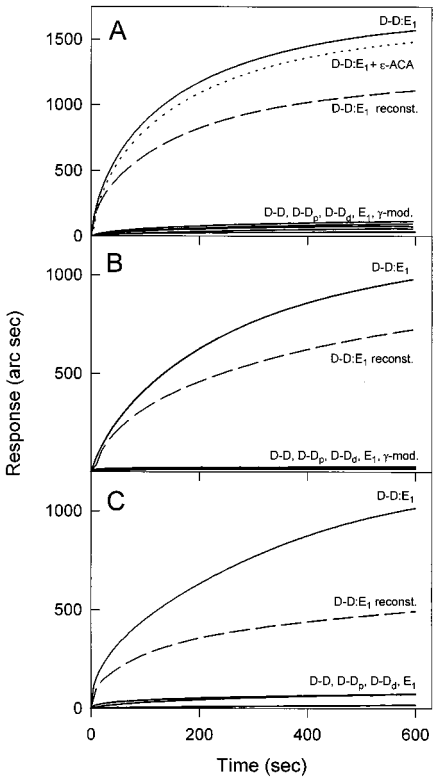

FIGURE 7: Analysis of binding of various fibrin-derived fragments and the D−D•E_1 complex to immobilized tPA (A), the anti-γ312−324 Mab (B), and the anti-Aα148−160 Mab (C) by surface plasmon resonance. The fragments and the complex were added at 1 μM, and their association was monitored in real time. The binding of the D−D•E_1 complex was substantially recovered after dissociation and reconstitution (broken lines in all panels). The binding of the complex to tPA in the presence of 100 mM ϵ-ACA is shown in panel A with the dotted line. The amount of binding observed with the E_1 fragment, the D−D fragment prepared from fibrin digest (D−D) and from the dissociated D−D•E_1 complex (D−D_d), the D−D fragment loaded with 0.4 mM GPRP and GHRP (D−D_p), and the γ-module (γ-mod.) was negligible in all cases.

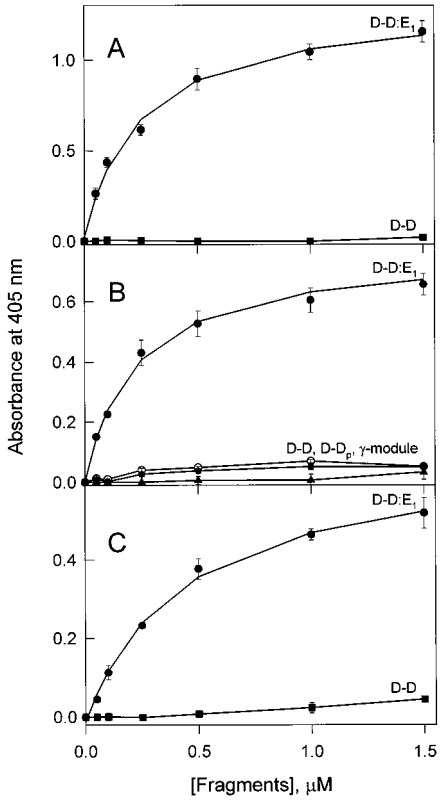

FIGURE 8: Analysis of binding of the fibrin-derived D−D fragment and the D−D•E_1 complex to immobilized tPA (A), the anti-γ312−324 Mab (B), and the anti-Aα148−160 Mab (C) by ELISA. Increasing concentrations of the D−D•E_1 complex (●), the D−D fragment (■), the peptide-loaded D−D fragment, D−D_p (○), and the γ-module (▲) were incubated with microtiter wells coated with tPA (A), the anti-γ312−324 Mab (B), and the anti-Aα148−160 Mab (C). Bound species were detected with the polyclonal antibody directed against the γ-module. Error bars reflect the standard deviation of three independent determinations. Curves drawn through the points are the best fits obtained as described in Experimental Procedures. The K_d for the tPA/D−D•E_1 interaction (A) was found to be 0.25 ± 0.03 μM.

shown), and the K_d of 0.6 μM was similar to those for D_Y and TSD (Table 2). In agreement with earlier observations (*38*, *50*), the binding was only slightly inhibited by 100 mM ϵ-ACA, suggesting that in the presence of this Lys analogue the binding occurs mainly via the γ312−324 binding sites that are Lys-independent. In similar experiments, the anti-γ312−324 Mab immobilized on a sensor chip did not exhibit noticeable binding of the D−D and E_1 fragments while it did bind the D−D•E_1 complex (Figure 7B). These findings were also confirmed in a sandwich ELISA in which the D−D•E_1 complex bound to immobilized tPA with a K_d of 0.25 μM, comparable to that determined by SPR, while the D−D fragment did not (Figure 8A and Table 2). Similarly, only the complex bound to the immobilized anti-γ312−324 Mab (Figure 8B). Thus, the γ312−324 epitope is not accessible in the D−D fragment and becomes available in the D−D•E_1 complex. It should be noted that the isolated recombinant γ-module also did not exhibit any binding in either SPR or ELISA (Figures 7B and 8B), in agreement with the fact that its fold is similar to that of the γ-module in the D fragment (*22*, *48*). In another set of experiments carried out with SPR and ELISA, the immobilized anti-Aα148−160 Mab did not exhibit binding with the D−D and E_1 fragments but did bind the D−D•E_1 complex, indicating that the Aα148−160 epitope is also exposed (Figures 7C and 8C). These experiments demonstrate directly that the DD•E interaction induces conformational changes in the D regions resulting in the exposure of their γ312−324 and Aα148−160 fibrin-specific epitopes.

Fibrin assembly is governed mainly by the DD•E interaction in which newly exposed polymerization sites A and B (knobs) of the E region starting with Gly-Pro-Arg (GPR) and Gly-His-Arg (GHR) sequences, respectively, interact with complementary binding sites a and b (holes) located in the γ- and β-modules, respectively, of the D regions of two other molecules (*8*). It was shown that synthetic peptides GPRP and GHRP mimicking these sequences bind to the complementary holes and may compete with the E regions, resulting in the dissociation of the D−D•E_1 complex (*55*). To answer the question of whether the interaction of these peptides with D−D is sufficient for the exposure of the fibrin-specific epitopes, we studied the effect of excess levels of these peptides on binding of the D−D fragment to immobilized tPA or the anti-γ312−324 and anti-Aα148−160 Mab by SPR and ELISA. Binding was not observed in any case (Figures 7 and 8B), indicating that the interaction of the peptides with the complementary holes is not sufficient to cause conformational changes and the exposure of the fibrin-specific epitopes in the D regions and that more

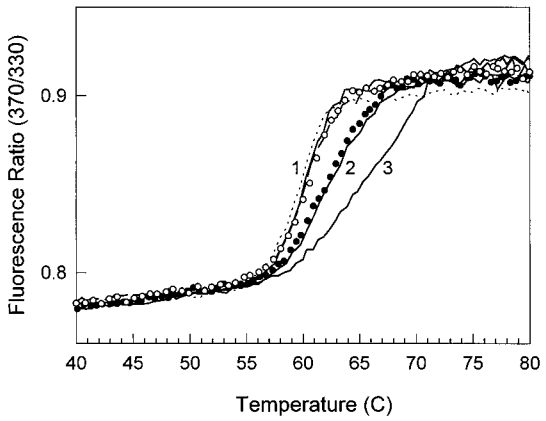

FIGURE 9: Fluorescence-detected thermal stability of the D region in fibrinogen, fibrin, and the isolated D−D fragment and its complex with the E_1 fragment. Curves 1 represent fluorescence-detected melting of fibrinogen and various fragments, while curves 2 and 3 represent the melting of the D−D·E_1 complex and polymeric fibrin, respectively. The curves for fibrinogen (···) and fragment D_1 (− − −), D−D (solid line 1), and D−D prepared from the D−D·E_1 complex (○) essentially coincide. The curves for the D−D·E_1 complex (solid line 2) and the reconstituted D−D·E_1 complex (●) also coincide. All experiments were performed in 50 mM glycine buffer (pH 8.6) with 0.5 mM Ca^{2+}.

extensive contacts between the D−D and E regions are required. In agreement, there is no substantial difference in the calculated solvent accessible surface areas of the two fibrin-specific epitopes in the D fragment and the D−D fragment loaded with GPRP and GHRP peptides (Table 1). This result is also in agreement with the previous findings that GPRP abolishes the stimulating effect of fibrin (*56*, *57*) and that fibrin monomers kept in a monomeric state by this peptide do not expose either fibrin-specific epitope (*21*, *56*).

Reversibility of the Exposure of the Fibrin-Specific Epitopes. To test if the conformational changes induced by the DD·E interaction are reversible, the D−D·E_1 complex was dissociated and reconstituted and the affinity of the reconstituted complex for immobilized tPA and anti-Aα148−160 and anti-γ312−324 Mabs was measured by SPR. Individual D−D and E_1 fragments purified from the acid-treated complex (see Experimental Procedures) showed no binding, indicating that the fibrin-specific epitopes in the D−D fragment were inaccessible after separation from the E_1 fragment (Figure 7). At the same time, the reconstituted complex exhibited substantial recovery of its binding to immobilized tPA and both Mabs (Figure 7) as well as most of its stimulating activity (not shown). These results indicate that both fibrin-specific epitopes were exposed after the reconstitution of the complex and that the conformational changes upon the DD·E interaction are reversible.

The DD·E Interaction Stabilizes the Conformation of the D−D Region. To further test the nature of these conformational changes, we compared the thermal stabilities of the D_1 and D−D fragments with that of the D−D·E_1 complex by heating them in the fluorometer while monitoring the ratio of fluorescence intensity at 370 nm to that at 330 nm as a measure of the spectral shift that accompanies unfolding. The D−D fragment exhibited a sigmoidal transition that is indistinguishable from that of the D_1 fragment or intact fibrinogen (Figure 9, curves 1). As shown previously (*5*), this transition is connected with the unfolding of the thermolabile domains in the D fragment, some of which are involved in the DD and DD·E interactions. The present result suggests that the end-to-end contacts in the D−D fragment do not affect noticeably the stability of these domains. The D−D·E_1 complex exhibited a broader transition centered at higher temperatures (Figure 9, solid curve 2), suggesting that the thermolabile domains are stabilized by the interaction with E_1, which itself is much more stable and unfolds at >80 °C (*3*). This stabilization was reversible since the D−D fragment that was purified from the acid-dissociated D−D·E_1 complex was also less stable [Figure 9 (○)] and became stable again after reconstitution of that complex [Figure 9 (●)]. However, the stability of the D−D fragment in the complex is not as great as in polymeric fibrin whose denaturation occurred at higher temperatures (Figure 9, curve 3). This is due to the fact that the DD·E interaction in the D−D·E_1 complex occurs via primary polymerization sites A and a, while an additional interaction via secondary sites B and b occurs in fibrin (*55*). Thus, the melting study indicates that the DD·E interaction stabilizes certain domains in the D regions. They also suggest that the D−D·E interaction via sites A and a, preserved in the D−D·E_1 complex, is only partially responsible for the stabilizing effect observed in fibrin; however, it is sufficient for the occurrence of the conformational changes that expose the fibrin-specific epitopes.

DISCUSSION

Conformational changes upon conversion of fibrinogen into fibrin result in the exposure of multiple sites that provide interaction of fibrin with different molecules and cell types. Although the importance of these changes is well-recognized, their mechanism remains unclear because of the absence of a high-resolution structure of fibrin. A possible approach to this problem may be to compare fibrinogen- and fibrin-derived fragments that might be expected to preserve the conformation and properties of the corresponding regions in fibrinogen and fibrin, respectively. Recent X-ray studies indicate that the fibrinogen-derived D fragment preserves the overall fold of the D regions of the parent molecule (*22*, *47*). At the same time, the conformation of this fragment differs only modestly from that of the same regions in the fibrin-derived dimeric D−D fragment (*22*). The question of whether such modest changes are sufficient for the exposure of new binding sites arises. In fact, the study presented here demonstrates that the fibrin-specific epitopes, Aα148−160 and γ312−324, are inaccessible in both the D and D−D fragments and that these fragments have similar thermal stabilities. In contrast, both epitopes were found to be exposed in the D−D·E_1 complex whose D−D component was found to be stabilized as in fibrin. Furthermore, the D−D·E_1 complex strongly stimulated the activation of plasminogen by tPA, as does fibrin, whereas the D and D−D fragments did not. These features of the D−D·E_1 complex were lost when the complex was dissociated under nondenaturing conditions and restored when the complex was reconstituted. These findings clearly indicate that it is the interaction with E_1 that stabilizes the D regions of the D−D fragment and induces the exposure of their fibrin-specific epitopes, whereas the conformation of these regions in the isolated D−D fragment resembles that in the monomeric D fragment and fibrinogen, in agreement with the X-ray studies.

Crystallographic data indicate that the γ312−324 region is located in a surface-oriented loop that is adjacent to the polymerization pocket (hole a) complementary to GPR knob A (*37*, *58*). Although the calculation of solvent accessibility revealed that this epitope is largely exposed in the D and D−D fragments, having only three residues buried, it was not accessible to tPA and the anti-γ312−324 Mab. This suggests that these three residues may be critical for binding and are exposed upon conversion of fibrinogen to fibrin. Alternatively, the already exposed region may rearrange to adopt an active fibrin-specific conformation. In either case, the conformational changes would occur within the γ-module. In contrast, the other epitope, Aα148−160, is situated on the coiled coil domain and is almost totally buried by the β-module and the fourth helix Aα166−195. Since the coiled coil is a rigid structure, one should not expect this epitope to be exposed by intradomain conformational changes as in the case of γ312−324. Rather, it requires the movement of those structural elements that cover it. Our calculations suggest that the removal of the fourth helix, proposed to be involved in the exposure (*22*), is not sufficient and that the β-module must also move away (dissociate) from the coiled coil domain to allow access to this region. The experiments with various fragments confirmed that proteolytic removal of the β-module results in the exposure of this epitope. Thus, the exposure of the two fibrin-specific epitopes seems to occur by different mechanisms, γ312−324 (tPA-binding site) by intradomain conformational changes in the γ-module and Aα148−160 (Pg/tPA-binding site) by the disruption of the interdomain interactions between the β-module (and possibly the fourth helix) and the coiled coil domain. Both of these events are triggered by the DD·E interaction.

The crystal structure of the D fragment shows that the Aα148−160 epitope of the coiled coil domain is situated far away from the γ-module where the A−a interaction occurs (Figure 1). The question of how an interaction in the γ-module causes conformational changes, namely, dissociation of the β-module from the coiled coil, in such a remote region arises. To clarify this question, the possible role of domain−domain interactions in these events may be considered. The interaction between individual domains in the D region was detected in studies of the denaturation of various D fragments in which it was demonstrated that removal of the γ-module results in destabilization of the β-module and that a single cleavage in the β-module causes destabilization of both β- and γ-modules (*25*, *26*, *59*). The interactions between the β- and γ-modules and between the β-module and the coiled coil domain were directly confirmed recently by crystallography (*22*). Finally, the results presented here show that removal of the γ-module is sufficient for the dissociation of the β-module from the coiled coil domain (Figures 2 and 3). Thus, if there is an interaction-dependent communication between domains in the D region, the conformational changes in the γ-module upon contact with E may modulate the interaction between the β-module and the coiled coil domain, resulting in their dissociation and the exposure of the Aα148−160 epitope.

The D−D·E-induced dissociation of the β-module from the coiled coil may also be connected with the two-stage character of the fibrin assembly process that includes formation of protofibrils and their lateral aggregation. The D−D·E interaction via primary polymerization sites A and a results in the formation of protofibrils, while the subsequent interaction via secondary polymerization sites B and b may promote the second stage, the lateral aggregation of protofibrils into thicker fibrils (*1*, *2*, *6*). The mechanism that governs this two-stage process is not known. Crystal structures of D−D variants revealed that the secondary polymerization site b (pocket) is situated in the β-module and consists of several residues, including Bβ Glu397 and Bβ Asp398 (*37*). In the D−D fragment, this site is not fully developed since the above-mentioned residues are pointed away from the pocket, while in the D−D fragment loaded with the GHRP peptide that mimics complementary site B, they undergo a flap movement to become a part of the pocket (*60*) (Figure 2C,D). Our analysis of side chain contacts in the D fragment indicates that the AαLys157 residue of the coiled coil domain interacts with Bβ Asp398, preventing the latter from moving to the pocket (Figure 2B,C). Obviously, this interaction must be disrupted upon dissociation of the β-module from the coiled coil and βAsp398 must be liberated to complete the formation of the polymerization pocket b that promotes lateral aggregation. On the basis of the evidence for extensive domain−domain interactions in the D region, we speculated earlier that the occupation of the primary polymerization sites during protofibril formation may cause an increased exposure of the secondary polymerization sites to enhance lateral aggregation of protofibrils (*25*). The results presented here are in good agreement with that speculation and allow a further clarification of the mechanism of this process.

On the basis of the foregoing results and discussion, one can suggest a possible scenario of events in the D regions upon fibrin assembly (Figure 10). The intermolecular DD·E interaction via primary polymerization sites A and a during protofibril formation causes conformational changes in the γ-module, resulting in its stabilization and exposure of its tPA-binding site that includes the γ312−324 region. These changes may modulate the intramolecular interaction between the β-module and the coiled coil domain, resulting in their dissociation and the disruption of the interaction between their Bβ Asp398 and AαLys157 residues. The β-module and the fourth helix move away from the coiled coil to open up access to the Aα148−160 Pg/tPA-binding site. The exposed tPA-binding site and Pg/tPA-binding site bind tPA and plasminogen, respectively, facilitating activation of the latter by the former. The liberated Bβ Asp398 undergoes movement to complete the formation of the secondary polymerization site (hole b) and to promote the interaction of the latter with complementary GHR knob B. The new conformation of the D−D region seems to be preserved in the D−D·E_1 complex, making it a more adequate model of fibrin than the D−D dimer. Obviously, the solution of the crystal structure of this complex would allow one not only to visualize the mode of interaction between complementary polymerization sites in fibrin but also to clarify the conformation of the D regions in fibrin and to elucidate the mechanisms of the conformational changes upon conversion of fibrinogen to fibrin in greater detail than presented here.

The D−D·E_1 complex accumulates upon degradation of cross-linked fibrin by plasmin (*27*). It was proposed that during thrombolytic therapy with tPA, activation of plasminogen on the D−D·E_1 surface results in systemic generation of plasmin, which degrades circulating fibrinogen thus reducing substantially the clot selectivity of tPA (*51*, *61*).

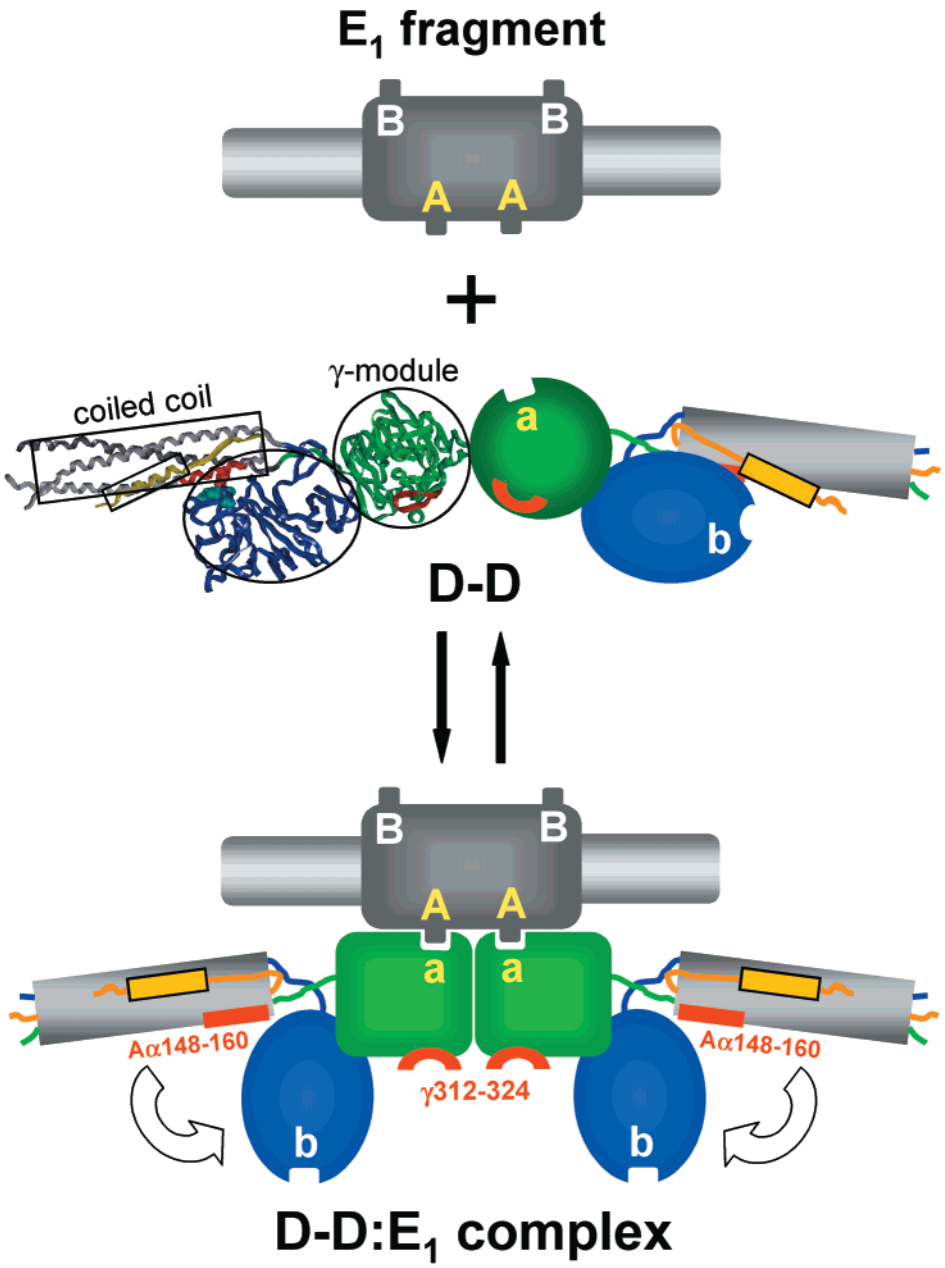

FIGURE 10: Schematic representation of the conformational changes in the D regions of fibrin and the D−D·E_1 complex upon their interaction with the E region. The coiled coil domains of the D and E regions are in gray; the fourth α-helix (Aα166−195) in the D region is in yellow, and the β- and γ-modules are in blue and green, respectively. The plasminogen/tPA-binding site (Aα148−160) and the tPA-binding site (γ312−324) are in red. A and a, and B and b, designate pairs of complementary polymerization sites. The dissociation of the β-module from the coiled coil domain is depicted by curved arrows.

On the basis of the observation that both the D−D·E_1 complex and fragment E bound to both plasminogen and tPA−Sepharose while isolated D−D did not, the stimulating effect of the complex was attributed to the ability of the E fragment in the complex to bind both tPA and plasminogen (*51*). The results presented here provide a different explanation for this phenomenon, namely, that the DD·E interaction induces reversible conformational changes in the D−D region resulting in the exposure of its tPA- and plasminogen-binding sites that are inactivated as soon as the complex dissociates (Figure 10). This mechanism suggests a possible approach to controlling the stimulating activity of the complex by its dissociation. In vivo, the dissociation is achieved by proteolytic conversion of the E_1 fragment to the E_3 fragment (*27*, *62*). This conversion occurs rapidly by cleavage in E_1 of the Bβ42−43 and Bβ53−54 bonds with plasmin (*62*, *63*) and seems to be involved in the regulation of fibrino(geno)-lysis. In vitro, the dissociation can be achieved in the presence of the GPRP peptide (*55*). This provides a useful hint for the search for effective dissociating agents that could be used upon therapeutic thrombolysis with tPA.

REFERENCES

1. Doolittle, R. F. (1984) *Annu. Rev. Biochem. 53*, 195−229.
2. Henschen, A., and McDonagh, J. (1986) in *Blood coagulation* (Zwaal, R. F. A., and Hemker, H. C., Eds.) pp 171−241, Elsevier Science Publishers, Amsterdam.
3. Privalov, P. L., and Medved, L. V. (1982) *J. Mol. Biol. 159*, 665−683.
4. Medved, L. V., Gorkun, O. V., and Privalov, P. L. (1983) *FEBS Lett. 160*, 291−295.

5. Medved, L., Litvinovich, S., Ugarova, T., Matsuka, Y., and Ingham, K. (1997) *Biochemistry 36*, 4685−4693.
6. Budzynski, A. Z. (1986) *Crit. Rev. Oncol. Hematol. 6*, 97−146.
7. Mosesson, M. W. (1998) *Semin. Thromb. Haemostasis 24*, 169−174.
8. Laudano, A. P., Cottrell, B. A., and Doolittle, R. F. (1983) *Ann. N.Y. Acad. Sci. 408*, 315−329.
9. Varadi, A., and Patthy, L. (1983) *Biochemistry 22*, 2440−2446.
10. Nieuwenhuizen, W. (1994) *Thromb. Res. 75*, 343−347.
11. Matsuka, Y. V., Medved, L. V., Brew, S. A., and Ingham, K. C. (1994) *J. Biol. Chem. 269*, 9539−9546.
12. Mosher, D. F., and Johnson, R. B. (1983) *Ann. N.Y. Acad. Sci. 408*, 583−594.
13. Bunce, L. A., Sporn, L. A., and Francis, C. W. (1992) *J. Clin. Invest. 89*, 842−850.
14. Bach, T. L., Barsigian, C., Yaen, C. H., and Martinez, J. (1998) *J. Biol. Chem. 273*, 30719−30728.
15. Zamarron, C., Ginsberg, M. H., and Plow, E. F. (1990) *Thromb. Haemostasis 64*, 41−46.
16. Zamarron, C., Ginsberg, M. H., and Plow, E. F. (1991) *J. Biol. Chem. 266*, 16193−16199.
17. Ugarova, T. P., Budzynski, A. Z., Shattil, S. J., Ruggeri, Z. M., Ginsberg, M. H., and Plow, E. F. (1993) *J. Biol. Chem. 268*, 21080−21087.
18. Tang, L., and Eaton, J. W. (1993) *J. Exp. Med. 178*, 2147−2156.
19. Tang, L., Ugarova, T. P., Plow, E. F., and Eaton, J. W. (1996) *J. Clin. Invest. 97*, 1329−1334.
20. Nieuwenhuizen, W., Vermond, A., Voskuilen, M., Traas, D. W., and Verheijen, J. H. (1983) *Biochim. Biophys. Acta 748*, 86−92.
21. Haddeland, U., Sletten, K., Bennick, A., Nieuwenhuizen, W., and Brosstad, F. (1996) *Thromb. Haemostasis 75*, 326−331.
22. Spraggon, G., Everse, S. J., and Doolittle, R. F. (1997) *Nature 389*, 455−462.
23. Deutsch, D. G., and Mertz, E. T. (1970) *Science 170*, 1095−1096.
24. Cierniewski, C. S., Kloczewiak, M., and Budzynski, A. Z. (1986) *J. Biol. Chem. 261*, 9116−9121.
25. Litvinovich, S. V., Henschen, A. H., Krieglstein, K. G., Ingham, K. C., and Medved, L. V. (1995) *Eur. J. Biochem. 229*, 605−614.
26. Medved, L. V., Litvinovich, S. V., and Privalov, P. L. (1986) *FEBS Lett. 202*, 298−302.
27. Olexa, S. A., and Budzynski, A. Z. (1979) *Biochemistry 18*, 991−995.
28. Belitser, V. A., Pozdnjakova, T. M., and Ugarova, T. P. (1980)-*Thromb. Res. 19*, 807−814.
29. Schielen, W. J. G., Voskuilen, M., Tesser, G. I., and Nieuwenhuizen, W. (1989) *Proc. Natl. Acad. Sci. U.S.A. 86*, 8951−8954.
30. Schielen, W. J. G., Adams, H. P. H. M., van Leuven, K., Voskuilen, M., Tesser, G. I., and Nieuwenhuizen, W. (1991) *Blood 77*, 2169−2173.
31. Ingham, K., and Brew, S. (1981) *Biochim. Biophys. Acta 670*, 181−189.
32. Verheijen, J. H., Mullaart, E., Chang, G. T., Kluft, C., and Wijngaards, G. (1982) *Thromb. Haemostasis 48*, 266−269.
33. Johnsson, B., Lofas, S., and Lindquist, G. (1991) *Anal. Biochem. 198*, 268−277.
34. Gorgani, N. N., Parish, C. R., Easterbrook Smith, S. B., and Altin, J. G. (1997) *Biochemistry 36*, 6653−6662.
35. Gorgani, N. N., Parish, C. R., and Altin, J. G. (1999) *J. Biol. Chem. 274*, 29633−29640.
36. Schuck, P., and Minton, A. P. (1996) *Trends Biochem. Sci. 21*, 458−460.
37. Everse, S. J., Spraggon, G., Veerapandian, L., Riley, M., and Doolittle, R. F. (1998) *Biochemistry 37*, 8637−8642.
38. Yonekawa, O., Voskuilen, M., and Nieuwenhuizen, W. (1992) *Biochem. J. 283*, 187−191.
39. Grailhe, P., Nieuwenhuizen, W., and Angles-Cano, E. (1994) *Eur. J. Biochem. 219*, 961−967.
40. Bosma, P. J., Rijken, D. C., and Nieuwenhuizen, W. (1988) *Eur. J. Biochem. 172*, 399−404.
41. de Munk, G. A., Caspers, G. T., Chang, P. H., Pouwels, B. E., Enger-Valk, J. H., and Verheijen, J. H. (1989) *Biochemistry 28*, 7318−7325.
42. Lezhen, T. I., Kudinov, S. A., and Medved, L. V. (1986) *FEBS Lett. 197*, 59−62.
43. Voskuilen, M., Vermond, A., Veeneman, G. H., van Boom, J. H., Klasen, E. A., Zegers, N. D., and Nieuwenhuizen, W. (1987) *J. Biol. Chem. 262*, 5944−5946.
44. Schielen, W. J. G., Voskuilen, M., Adams, H. P. H. M., Tesser, G. I., and Nieuwenhuizen, W. (1990) *Blood Coagulation Fibrinolysis 1*, 521−524.
45. Schielen, W. J. G., Adams, H. P. H. M., Voskuilen, M., Tesser, G. I., and Nieuwenhuizen, W. (1991) *Biochem. J. 276*, 655−659.
46. Schielen, W. J. G., Adams, H. P. H. M., Voskuilen, M., Tesser, G. I., and Nieuwenhuizen, W. (1993) *Fibrinolysis 7*, 63−67.
47. Brown, J. H., Volkmann, N., Jun, G., Henschen-Edman, A. H., and Cohen, C. (2000) *Proc. Natl. Acad. Sci. U.S.A. 97*, 85−90.
48. Yee, V. C., Pratt, K. P., Cote, H. C. F., Le Trong, I., Chung, D. W., Davie, E. W., Stenkamp, R. E., and Teller, D. C. (1997) *Structure 5*, 125−138.
49. Verheijen, J. H., Nieuwenhuizen, W., and Wijngaards, G. (1982) *Thromb. Res. 27*, 377−385.
50. Hasan, A. A. K., Chang, W. S., and Budzynski, A. Z. (1992) *Blood 79*, 2313−2321.
51. Weitz, J. I., Leslie, B., and Ginsberg, J. (1991) *J. Clin. Invest. 87*, 1082−1090.
52. Druzhyna, N. N., Makogonenko, E. M., and Yakovlev, S. A. (1997) *Thromb. Res. 87*, 131−139.
53. Haddeland, U., Bennick, A., and Brosstad, F. (1994) *Blood Coagulation Fibrinolysis 5*, 767−772.
54. Mosesson, M. W., Siebenlist, K. R., Voskuilen, M., and Nieuwenhuizen, W. (1998) *Thromb. Haemostasis 79*, 796−801.
55. Moskowitz, K. A., and Budzynski, A. Z. (1994) *Biochemistry 33*, 12937−12944.
56. Suenson, E., and Petersen, L. C. (1986) *Biochim. Biophys. Acta 870*, 510−519.
57. Kaczmarek, E., Lee, M. H., and McDonagh, J. (1993) *J. Biol. Chem. 268*, 2474−2479.
58. Pratt, K. P., Cote, H. C., Chung, D. W., Stenkamp, R. E., and Davie, E. W. (1997) *Proc. Natl. Acad. Sci. U.S.A. 94*, 7176−7181.
59. Medved, L. V., Platonova, T. N., Litvinovich, S. V., and Lukinova, N. I. (1988) *FEBS Lett. 232*, 56−60.
60. Everse, S. J., Spraggon, G., Veerapandian, L., and Doolittle, R. F. (1999) *Biochemistry 38*, 2941−2946.
61. Weitz, J. I., Stewart, R. J., and Fredenburg, J. C. (1999) *Thromb. Haemostasis 82*, 974−982.
62. Olexa, S. A., Budzynski, A. Z., Doolittle, R. F., Cottrell, B. A., and Greene, T. C. (1981) *Biochemistry 20*, 6139−6145.
63. Takagi, T., and Doolittle, R. F. (1975) *Biochemistry 14*, 940−946.

BI001847A